

Superconductivity at 15.6 K in Calcium-doped $\text{Tb}_{1-x}\text{Ca}_x\text{FeAsO}$: the structure requirement for achieving superconductivity in the hole-doped 1111 phase

Gang Mu, Bin Zeng, Peng Cheng, Xiyu Zhu, Fei Han, Bing Shen, and Hai-Hu Wen*

National Laboratory for Superconductivity, Institute of Physics and Beijing National Laboratory for Condensed Matter Physics, Chinese Academy of Sciences, P. O. Box 603, Beijing 100190, People's Republic of China

Superconductivity at about 15.6 K was achieved in $\text{Tb}_{1-x}\text{Ca}_x\text{FeAsO}$ by partially substituting Tb^{3+} with Ca^{2+} in the nominal doping region $x = 0.40 \sim 0.50$. A detailed investigation was carried out in a typical sample with doping level of $x = 0.44$. The upper critical field of this sample was estimated to be 77 Tesla from the magnetic field dependent resistivity data. The domination of hole-like charge carriers in the low-temperature region was confirmed by Hall effect measurements. The comparison between the calcium-doped sample $\text{Pr}_{1-x}\text{Ca}_x\text{FeAsO}$ (non-superconductive) and the Strontium-doped sample $\text{Pr}_{1-x}\text{Sr}_x\text{FeAsO}$ (superconductive) suggests that a larger ion radius of the doped alkaline-earth element compared with that of the rare-earth element may be a necessary requirement for achieving superconductivity in the hole-doped 1111 phase.

PACS numbers: 74.10.+v, 74.70.Dd, 74.25.Fy, 74.62.Dh

I. INTRODUCTION

The discovery of superconductivity in iron pnictides have generated enormous interests in the community of condensed matter physics.¹ Up to date, the iron pnictide superconductors have developed into several families with different structures, which were abbreviated as the 1111 phase (including the oxy-arsenide¹ and fluorine-arsenide²), 122 phase,^{3,4} 111 phase,^{5,6,7} 11 phase,⁸ 42622 phase,⁹ and so on. It seems that each phase with different structure has a unique superconducting transition temperature T_c . As for the 1111 phase, most of the discovered superconductors are characterized as electron-doped ones^{10,11,12,13,14}, while the hole-doped superconductors were only reported in the strontium-doped $\text{Ln}_{1-x}\text{Sr}_x\text{FeAsO}$ ($\text{Ln} = \text{La}, \text{Pr}, \text{Nd}$).^{15,16,17,18} The hole-doped superconductivity in 1111 phase by substituting other ion-dopants with valence of "+2", such as barium or calcium, seems quite difficult to be achieved, at least in many of the rare-earth based systems. Obviously, it is important to carry out more explorations in this direction in order to extend the family of the hole-doped superconductors in 1111 phase. And it is also significant to investigate the factors which govern the electronic properties (superconducting or non-superconducting) in the hole-doped side based on the 1111 phase.

In this paper we report a new hole-doped superconductor in the 1111 phase, calcium-doped $\text{Tb}_{1-x}\text{Ca}_x\text{FeAsO}$, with the maximum superconducting transition temperature of 15.6 K (95% ρ_n). It is found that superconductivity appears in the nominal doping region $x = 0.40 \sim 0.50$. The physical properties of a selected sample with $x = 0.44$ were investigated in depth. We estimated the upper critical field of this sample to be 77 Tesla based on the Werthamer-Helfand-Hohenberg (WHH) formula.¹⁹ The conducting charge carriers in this sample were characterized to be hole type in a wide low-temperature region by the Hall effect measurements. Meanwhile, we have also successfully synthesized calcium-doped $\text{Pr}_{1-x}\text{Ca}_x\text{FeAsO}$,

which also displays hole-type charge carriers in low-temperature region but doesn't superconduct at all. We attribute this different behavior to the sensitive electronic response to the relative radii of the doped ions compared with that of the rare-earth ions.

II. EXPERIMENTAL DETAILS

The $\text{Tb}_{1-x}\text{Ca}_x\text{FeAsO}$ samples were prepared using a two-step solid state reaction method. In the first step, TbAs and CaAs were prepared by reacting Tb flakes (purity 99.99%), Ca flakes (purity 99.9%) and As grains (purity 99.99%) at 500 °C for 10 hours and then 700 °C for 16 hours. They were sealed in an evacuated quartz tube when reacting. Then the resultant precursors were thoroughly grounded together with Fe powder (purity 99.95%) and Fe_2O_3 powder (purity 99.5%) in stoichiometry as given by the formula $\text{Tb}_{1-x}\text{Ca}_x\text{FeAsO}$. All the weighing and mixing procedures were performed in a glove box with a protective argon atmosphere. Then the mixtures were pressed into pellets and sealed in an evacuated quartz tube. The materials were heated up to 1150-1170 °C with a rate of 120 °C/hr and maintained for 40 hours. Then a cooling procedure was followed. After that, we can get the superconducting polycrystalline samples. The process of preparing $\text{Pr}_{1-x}\text{Ca}_x\text{FeAsO}$ samples is quite similar to that of $\text{Tb}_{1-x}\text{Ca}_x\text{FeAsO}$.

The x-ray diffraction (XRD) measurements of our samples were carried out by a *Mac-Science* MXP18A-HF equipment with Cu-K_α radiation. The ac susceptibility of the samples were measured on the MagLab-12T (Oxford) with an ac field of 0.1 Oe and a frequency of 333 Hz. The resistance and Hall effect measurements were done using a six-probe technique on the Quantum Design instrument physical property measurement system (PPMS) with magnetic fields up to 9 T. The current direction was changed for measuring each point in order to remove the contacting thermal power. The temperature

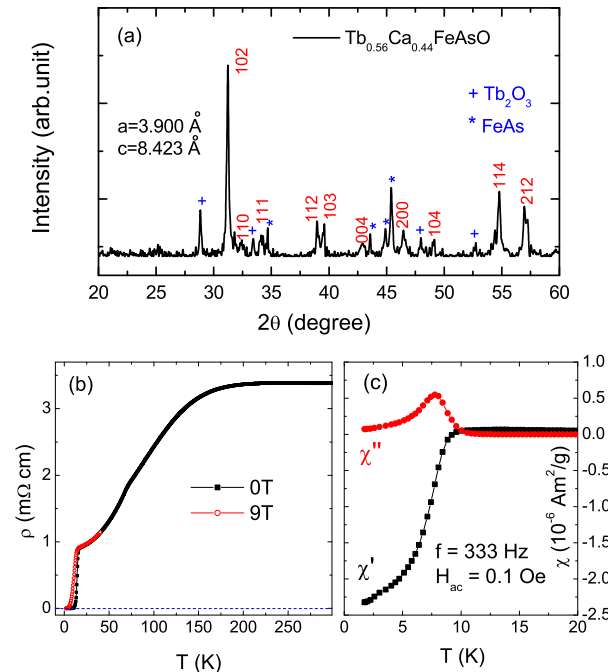


FIG. 1: (Color online) (a) X-ray diffraction pattern for the sample $\text{Tb}_{0.56}\text{Ca}_{0.44}\text{FeAsO}$. All the main peaks can be indexed to the tetragonal ZrCuSiAs -type structure. The peaks from the impurities are precisely indexed to Tb_2O_3 and FeAs . (b) Temperature dependence of resistivity for the $\text{Tb}_{0.56}\text{Ca}_{0.44}\text{FeAsO}$ sample under two different fields 0 T and 9 T. The data under 0 T is shown up to 300 K. (c) The ac susceptibility data measured with $f = 333$ Hz and $H_{ac} = 0.1$ Oe.

stabilization was better than 0.1% and the resolution of the voltmeter was better than 10 nV.

III. EXPERIMENTAL DATA AND DISCUSSION

A. Sample characterization for $\text{Tb}_{0.56}\text{Ca}_{0.44}\text{FeAsO}$

The x-ray diffraction pattern for the sample $\text{Tb}_{1-x}\text{Ca}_x\text{FeAsO}$ with the nominal doping level of $x = 0.44$ is shown in Fig. 1(a). It is clear that all the main peaks can be indexed to the 1111 phase with the tetragonal ZrCuSiAs -type structure.²⁰ The main impurity phases were identified to be Tb_2O_3 and FeAs , which are all not superconducting in the measuring temperature. By using the software Fullprof, we can determine the lattice constants as $a = 3.900$ Å and $c = 8.423$ Å for this sample. By comparing with the lattice constants of the parent phase TbFeAsO ($a = 3.898$ Å, $c = 8.404$ Å) reported by other group,²¹ we find that the a -axis lattice constant in the present sample is slightly larger than that of the parent phase, while the expansion along

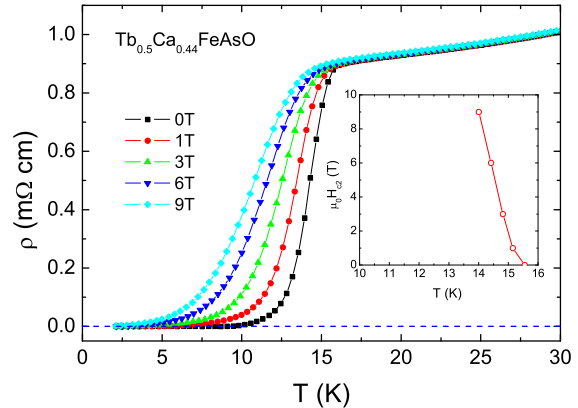


FIG. 2: (Color online) Temperature dependence of resistivity for $\text{Tb}_{0.56}\text{Ca}_{0.44}\text{FeAsO}$ near the superconducting transition under different magnetic fields. The onset transition temperature defined by $95\%\rho_n$ shifts with the magnetic field slowly. Inset: phase diagram derived from the resistive transition curves.

the c -axis direction is more distinct. In fact, the similar tendency has been observed in other hole-doped systems in the 1111 phase.^{16,17} This indicates that the calcium atoms go into the crystal lattice of the TbFeAsO system because the radius of Ca^{2+} is larger than that of Tb^{3+} (see Fig. 7).

In Fig. 1(b) we present a typical set of resistive data for the same sample $\text{Tb}_{0.56}\text{Ca}_{0.44}\text{FeAsO}$ under 0 T and 9 T. The data under 0 T is shown up to 300 K. A clear superconducting transition can be seen in the low temperature region. Taking a criterion of $95\%\rho_n$, the onset transition temperature is determined to be 15.6 K. A magnetic field of 9 T only suppresses the onset transition temperature about 1.6 K, indicating a rather high upper critical field in our sample. In the high temperature region, the resistivity anomaly coming from the antiferromagnetic (AF) or structural transition has been suppressed and a flattening feature was observed clearly. The similar behavior has been observed in other hole-doped 1111 systems $\text{Ln}_{1-x}\text{Sr}_x\text{FeAsO}$ ($\text{Ln} = \text{La}, \text{Pr}, \text{Nd}$).^{15,16,17,18} Figure 1(c) shows the ac susceptibility data measured with $f = 333$ Hz and $H_{ac} = 0.1$ Oe. A rough estimate from the diamagnetic signal shows that the superconducting volume fraction of the present sample is beyond 50%, confirming the bulk superconductivity in our samples. The onset critical temperature by magnetic measurements is roughly corresponding to the zero-resistance temperature.

B. Upper critical field for $\text{Tb}_{0.56}\text{Ca}_{0.44}\text{FeAsO}$

We attempted to estimate the upper critical field of the sample $\text{Tb}_{0.56}\text{Ca}_{0.44}\text{FeAsO}$ from the resistivity data.

C. Hall effect of $\text{Tb}_{1-x}\text{Ca}_x\text{FeAsO}$

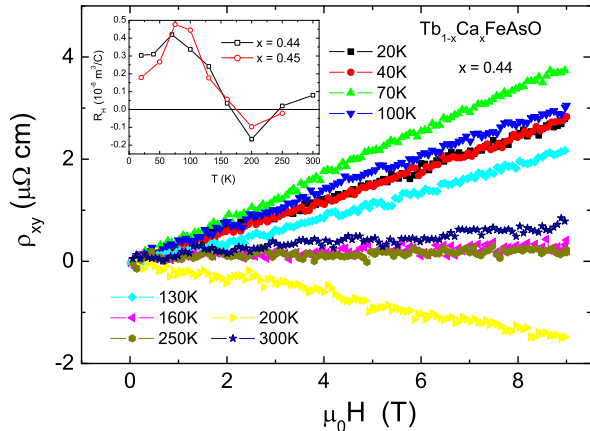


FIG. 3: (Color online) Hall effect measurements for the samples $\text{Tb}_{1-x}\text{Ca}_x\text{FeAsO}$. The main frame shows the field dependence of the Hall resistivity ρ_{xy} at different temperatures for the sample with $x = 0.44$. Inset: Temperature dependence of the Hall coefficient R_H for two samples with $x = 0.44$ and 0.45 .

Temperature dependence of resistivity under different magnetic fields is shown in the main frame of Fig. 2. It is found that the onset transition point, which reflects mainly the upper critical field in the configuration of $\text{H} \parallel \text{ab-plane}$, shifts more slowly than the zero resistivity point to low temperatures under fields. The magnetoresistance in the normal state is found to be quite small. We take a criterion of $95\% \rho_n$ to determine the onset transition points under different fields, which are represented by the red open circles in the inset of Fig. 2. From these data we can determine the slope of $H_{c2}(T)$ near T_c , $dH_{c2}/dT|_{T_c} \approx -7.1 \text{ T/K}$. By using the WHH formula¹⁹ the value of zero temperature upper critical field $H_{c2}(0)$ can be estimated through:

$$H_{c2}(0) = -0.693T_c \left(\frac{dH_{c2}}{dT} \right) |_{T_c}. \quad (1)$$

Taking $T_c = 15.6 \text{ K}$, we get $H_{c2}(0) \approx 77 \text{ T}$. Regarding the relatively low value of $T_c = 15.6 \text{ K}$ in the present sample, this value of upper critical field $H_{c2}(0)$ is actually quite high.

Actually, in the strontium-doped $\text{Ln}_{1-x}\text{Sr}_x\text{FeAsO}$ ($\text{Ln} = \text{La}, \text{Pr}$), the rather high $H_{c2}(0)$ and large slope $dH_{c2}(T)/dT|_{T_c}$ ($\sim 4 \text{ T/K}$) have been observed when comparing with the F-doped LaFeAsO sample, which was attributed to higher quasiparticle density of states (DOS) near the Fermi level in the hole-doped samples.¹⁷ Surprisingly, the slope $dH_{c2}(T)/dT|_{T_c}$ found here is even larger than that of the strontium-doped samples. The essential physical mechanism for this behavior may still need more investigation in this system, including that from the theoretical side.

It is known that Hall effect measurement is a useful tool to investigate the information of charge carriers and the band structure. For a conventional metal with Fermi liquid feature, the Hall coefficient is almost independent of temperature. However, this situation is changed for a multiband material²² or a sample with non-Fermi liquid behavior, such as the cuprate superconductors.²³ To examine the type of the conducting carriers, we measured the Hall effect of the samples $\text{Tb}_{1-x}\text{Ca}_x\text{FeAsO}$. The main frame of Fig. 3 shows the magnetic field dependence of Hall resistivity (ρ_{xy}) at different temperatures for the sample with $x = 0.44$. In the experiment ρ_{xy} was taken as $\rho_{xy} = [\rho(+H) - \rho(-H)]/2$ at each point to eliminate the effect of the misaligned Hall electrodes. We can see that all curves in Fig. 3 have good linearity versus the magnetic field. Moreover, ρ_{xy} is positive at all temperatures below 160 K giving a positive Hall coefficient $R_H = \rho_{xy}/H$, which actually indicates that hole-type charge carriers dominate the conduction below 160 K in the present sample.

The temperature dependence of R_H for two samples with $x = 0.44$ and 0.45 is shown in the inset of Fig. 3. One can see that the evolution of R_H with temperature are quite similar for the two samples, indicating the reliability of the Hall data. The hump feature in low temperature region is quite similar to that observed in strontium-doped $\text{Ln}_{1-x}\text{Sr}_x\text{FeAsO}$ ($\text{Ln} = \text{La}, \text{Pr}$) samples.^{15,16,17} However, there is still some differences obviously. Firstly, the Hall coefficient R_H changes its sign at about 160 K which is remarkably lower than that observed in the strontium-doped systems ($\sim 250 \text{ K}$). This character seems to be quite common in the calcium-doped 1111 phase because the sign changing of R_H was also found to occur at about 160 K in $\text{Pr}_{1-x}\text{Ca}_x\text{FeAsO}$ (see Fig. 5) and $\text{Nd}_{1-x}\text{Ca}_x\text{FeAsO}$ (data not shown here). Secondly, the negative R_H at about 200 K has a rather large absolute value. This feature seems to be unique in the calcium-doped superconducting samples, since it can't be observed in $\text{Ln}_{1-x}\text{Sr}_x\text{FeAsO}$ ($\text{Ln} = \text{La}, \text{Pr}$) or $\text{Pr}_{1-x}\text{Ca}_x\text{FeAsO}$. Assuming a simple two-band scenario with different types of carriers, we can express the Hall coefficient R_H in the low-field limit as

$$R_H = \frac{\sigma_1 \mu_1 + \sigma_2 \mu_2}{(\sigma_1 + \sigma_2)^2}, \quad (2)$$

where σ_i and μ_i are the conductivity and the mobility of the i^{th} band, respectively. They are determined by the charge-carrier density and scattering rate of each band. We attribute the strong and complicated temperature dependence of R_H in the present system to the competing effect of the scattering rate as well as the charge-carrier density in different bands.

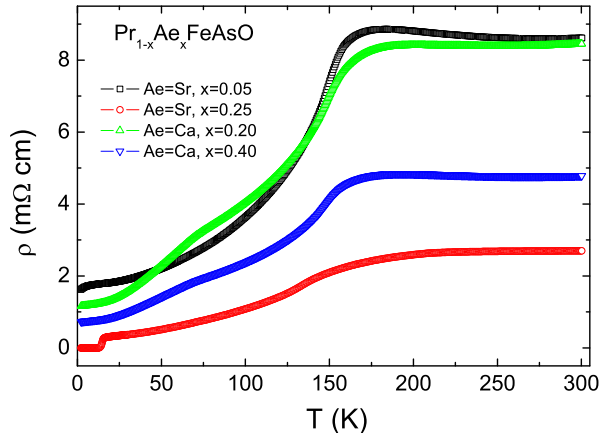


FIG. 4: (Color online) Temperature dependence of resistivity for two calcium-doped samples $\text{Pr}_{1-x}\text{Ca}_x\text{FeAsO}$ with $x = 0.20$ and 0.40 , along with two strontium-doped samples $\text{Pr}_{1-x}\text{Sr}_x\text{FeAsO}$ with $x = 0.05$ and 0.25 for comparison. It is clear that the behavior of the calcium-doped samples is between that of the two strontium-doped samples in high temperature region.

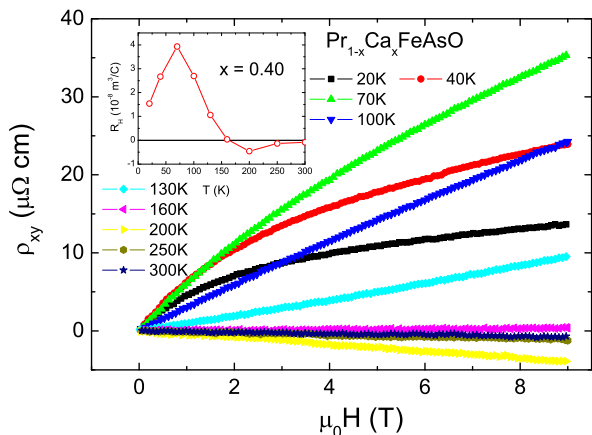


FIG. 5: (Color online) Hall effect measurements for one sample $\text{Pr}_{0.60}\text{Ca}_{0.40}\text{FeAsO}$. The main frame shows the field dependence of the Hall resistivity ρ_{xy} at different temperatures. Inset: Temperature dependence of the Hall coefficient R_H , which is positive in the temperature region below about 160 K.

D. The case in the calcium-doped $\text{Pr}_{1-x}\text{Ca}_x\text{FeAsO}$

One may be curious to know what would happen if we substitute calcium to the systems based on other rare-earth elements. Actually, we have tried the case of calcium-doped LaFeAsO , PrFeAsO , NdFeAsO , GdFeAsO , and so on. Here we just show the results

of $\text{Pr}_{1-x}\text{Ca}_x\text{FeAsO}$ for example. No superconductivity was found in the calcium-doped $\text{Pr}_{1-x}\text{Ca}_x\text{FeAsO}$ samples in quite wide doping range ($0.10 \leq x \leq 0.50$). In Fig. 4, we show the temperature dependence of resistivity for two selected samples with $x = 0.20$ and 0.40 . In order to have a comparison, we also display the resistivity data for two strontium-doped $\text{Pr}_{1-x}\text{Sr}_x\text{FeAsO}$ samples with different doping levels ($x = 0.05$ and 0.25). It is clear that the resistivity anomaly from the AF or structural transition around 160 K is suppressed gradually with the increase of strontium contents. By having a closer scrutiny, we find that the behavior of the calcium-doped samples is between that of the two strontium-doped samples in high temperature region. This may suggest that the real doped charge carriers in the calcium-doped PrFeAsO are roughly corresponding to $0.10 \sim 0.20$ of that of the strontium-doped PrFeAsO system and the AF order has been suppressed to a certain extent by the calcium-doping.

To further investigate the conducting properties of the $\text{Pr}_{1-x}\text{Ca}_x\text{FeAsO}$ sample, we have measured the Hall effect of them and display the data of one typical sample with $x = 0.40$ in Fig. 5. Nonlinear behavior was observed in the field dependent ρ_{xy} data below 100 K. The hump feature and positive value of R_H can be seen below about 160 K, which is rather similar to that observed in $\text{Tb}_{1-x}\text{Ca}_x\text{FeAsO}$ (see Fig. 3). This behavior indicates strongly that the hole-type charge carriers have been induced to the system and they dominate the conducting in low temperature region.

In order to find the factors which prevent $\text{Pr}_{1-x}\text{Ca}_x\text{FeAsO}$ from superconducting even if hole-type charge carriers have been doped into the system, we analyzed the structural details of one calcium-doped $\text{Pr}_{1-x}\text{Ca}_x\text{FeAsO}$ with nominal $x = 0.4$. Selected Rietveld refinement results are listed in table I, and the refinement pattern is shown in Fig. 6. Only small amounts of Pr_2O_3 and FeAs can be seen as the impurities. From the refinement, we find that the actual doping concentration for the sample $\text{Pr}_{1-x}\text{Ca}_x\text{FeAsO}$ with nominal $x = 0.4$ is only about 0.13, which is quite consistent with the argument we obtained from the resistivity data (see Fig. 4). In order to have a comparison with the strontium-doped PrFeAsO system where superconductivity has been obtained, we also display the structural parameters of the parent phase PrFeAsO and strontium-doped $\text{Pr}_{1-x}\text{Sr}_x\text{FeAsO}$ with $x = 0.16$ (the value from refinement)^{24,25} in table I. Here we define d_{PrOPr} and d_{AsFeAs} as the vertical distance between the Pr atoms residing at the top and bottom of the PrO layer and that between the As atoms in the FeAs layer, respectively. And d_{inter} is the interlayer space between the Pr-O-Pr block and the As-Fe-As block. It is clear that the lattice constant along a -axis remains nearly unchanged while that along c -axis expands clearly when calcium is doped to PrFeAsO . Both d_{PrOPr} and d_{AsFeAs} shrink slightly while d_{inter} expands distinctly with the actual calcium doping of 0.13, resulting in the expansion

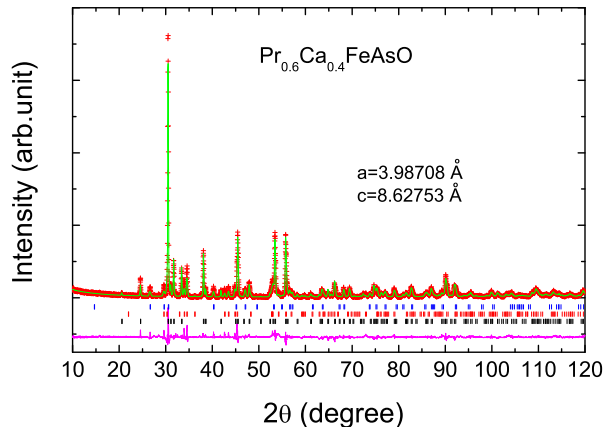


FIG. 6: (Color online) The observed (red crosses) and calculated (green solid line) x-ray powder diffraction patterns of $\text{Pr}_{0.6}\text{Ca}_{0.4}\text{FeAsO}$. The three rows of vertical bars show the calculated positions of Bragg reflections for Pr_2O_3 (blue), FeAs (red) and $\text{Pr}_{0.6}\text{Ca}_{0.4}\text{FeAsO}$ (black), respectively. The magenta solid line shown at the bottom of the figure indicates the differences between observations and calculations.

behavior of the lattice along c -axis. Surprisingly, we find that calcium doping gives a rather similar influence to the crystal structure to that of strontium doping, when we compare the parameters of $\text{Pr}_{0.87}\text{Ca}_{0.13}\text{FeAsO}$ and $\text{Pr}_{0.84}\text{Sr}_{0.16}\text{FeAsO}$ as shown in table I, even if the radius of Ca^{2+} is smaller than that of Pr^{3+} while the radius of Sr^{2+} is larger (see Fig. 7). We note that the sample $\text{Pr}_{0.84}\text{Sr}_{0.16}\text{FeAsO}$ still doesn't superconduct and superconductivity was achieved in the samples with even higher doping, as reported in Ref.[25]. However, the fact that the radius of Ca^{2+} is smaller than that of Pr^{3+} seems to prevent from doping even more calcium to PrFeAsO and consequently prevent from achieving superconductivity in $\text{Pr}_{1-x}\text{Ca}_x\text{FeAsO}$ system, because the effect of doped calcium is to expand the lattice along c -axis. This argument is reinforced by the fact that only 13% of calcium can be doped into the system even if the nominal doping concentration is 40%.

To validate our supposition, we have tried the case of other calcium-doped samples. In $\text{La}_{1-x}\text{Ca}_x\text{FeAsO}$, we found that it is quite difficult to dope charge carriers (probably also Ca) to the system and the Hall coefficient remains negative, and very similar behaviors to that of $\text{Pr}_{1-x}\text{Ca}_x\text{FeAsO}$ were observed in $\text{Nd}_{1-x}\text{Ca}_x\text{FeAsO}$. Very small superconducting signal can be observed in $\text{Sm}_{1-x}\text{Ca}_x\text{FeAsO}$ sometimes. Zero resistance can be obtained easily in $\text{Gd}_{1-x}\text{Ca}_x\text{FeAsO}$, but the diamagnetic signal is smaller than that of the $\text{Tb}_{1-x}\text{Ca}_x\text{FeAsO}$ system. We can't get the 1111 phase on the heavy rare-earth (Dy, Ho, et al) side under ambient pressure. By summarizing the phenomena mentioned above, we argue that the relationship between the ion radii of the rare-

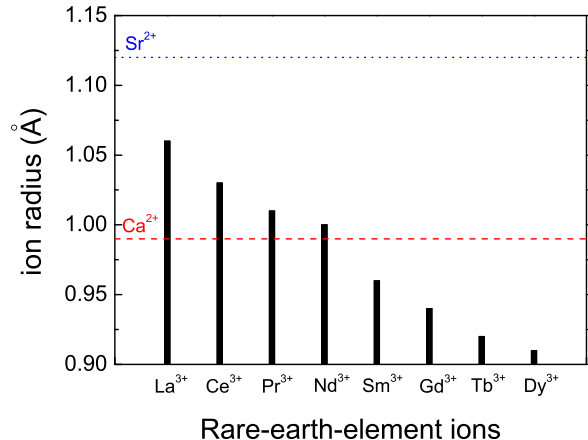


FIG. 7: (Color online) The data of ion radii for some selected rare-earth-element ions. The blue dotted and red dashed lines represent the value of Sr^{2+} and Ca^{2+} , respectively.

earth elements and the alkaline-earth element may play a key role in achieving superconductivity in the hole-doped 1111 phase (see Fig. 7). That is, superconductivity emerges only when the ion radius of the rare-earth element is smaller than that of the alkaline-earth element. At this time, we can say safely that it is rather difficult, if not impossible, to obtain superconductivity when the ion radius of the rare-earth element is larger. Moreover, it seems that superconductivity favors the situation when the difference between the two radii is larger, within the tolerance of crystal lattice. These arguments are quite consistent with that stated in the previous paragraph. This actually gives a restriction in exploring new superconductors in hole-doped side of 1111 phase.

IV. CONCLUDING REMARKS

In summary, bulk superconductivity was achieved by substituting Tb^{3+} with Ca^{2+} in TbFeAsO system. The maximum superconducting transition temperature $T_c = 15.6$ K is found to appear around the nominal doping level $x = 0.40 \sim 0.50$. The positive Hall coefficient R_H in a wide low-temperature range suggests that the hole-type charge carriers dominate the conduction in this system. Surprisingly, the slope of the upper critical magnetic field vs. temperature near T_c in calcium-doped $\text{Tb}_{1-x}\text{Ca}_x\text{FeAsO}$ is found to be much higher than that of the electron-doped and strontium-doped ones. Moreover, we have investigated the structural and conducting properties of other calcium-doped systems (taking $\text{Pr}_{1-x}\text{Ca}_x\text{FeAsO}$ for example). We found that the relationship between the ion radii of the rare-earth elements and alkaline-earth elements may play a key role in achieving superconductivity in the hole-doped 1111

phase.

Acknowledgments

We acknowledge the help of XRD experiments from L. H. Yang and H. Chen. This work is supported by the Nat-

ural Science Foundation of China, the Ministry of Science and Technology of China (973 project: 2006CB01000, 2006CB921802), the Knowledge Innovation Project of Chinese Academy of Sciences (ITSNEM).

-
- * Electronic address: hhwen@aphy.iphy.ac.cn
- ¹ Y. Kamihara, T. Watanabe, M. Hirano, and H. Hosono, *J. Am. Chem. Soc.* **130**, 3296 (2008).
 - ² X. Zhu, F. Han, P. Cheng, G. Mu, B. Shen, and H. H. Wen, *Europhys. Lett.* **85**, 17011 (2009).
 - ³ M. Rotter, M. Tegel, and D. Johrendt, *Phys. Rev. Lett.* **101**, 107006 (2008).
 - ⁴ K. Sasmal, B. Lv, B. Lorenz, A. M. Guloy, F. Chen, Y. Y. Xue, and C. W. Chu, *Phys. Rev. Lett.* **101**, 107007 (2008).
 - ⁵ X. C. Wang, Q. Q. Liu, Y. X. Lv, W. B. Gao, L. X. Yang, R. C. Yu, F. Y. Li, and C. Q. Jin, arXiv: Condmat/0806.4688.
 - ⁶ J. H. Tapp, Z. Tang, B. Lv, K. Sasmal, B. Lorenz, P. C. W. Chu, and A. M. Guloy, *Phys. Rev. B* **78**, 060505(R) (2008).
 - ⁷ M. J. Pitcher, D. R. Parker, P. Adamson, S. J. C. Herkelrath, A. T. Boothroyd, and S. J. Clarke, *Chem. Commun. (Cambridge)* **2008**, 5918.
 - ⁸ F.C. Hsu, J.Y. Luo, K.W. Yeh, T.K. Chen, T.W. Huang, P.M. Wu, Y.C. Lee, Y.L. Huang, Y.Y. Chu, D.C. Yan, M.K. Wu, *Proceedings of National Academy of Sciences* **105**, 14262 (2008).
 - ⁹ X. Zhu, F. Han, G. Mu, P. Cheng, B. Shen, B. Zeng, and H. H. Wen, *Phys. Rev. B* **79**, 220512(R) (2009)
 - ¹⁰ Z. Ren, J. Yang, W. Lu, W. Yi, G. C. Che, X. L. Dong, L. L. Sun, and Z. X. Zhao, *Materials Research Innovations* **12**, 105, (2008).
 - ¹¹ P. Cheng, L. Fang, H. Yang, X. Zhu, G. Mu, H. Luo, Z. Wang, and H. H. Wen, *Science in China G*, **51**(6), 719-722 (2008).
 - ¹² C. Wang, L. Li, S. Chi, Z. Zhu, Z. Ren, Y. Li, Y. Wang, X. Lin, Y. Luo, S. Jiang, X. Xu, G. Cao, and Z. Xu, *Europhys. Lett.* **83**, 67006 (2008).
 - ¹³ A. S. Sefat, A. Huq, M. A. McGuire, R. Jin, B. C. Sales, D. Mandrus, L. M. D. Cranswick, P. W. Stephens, and K. H. Stone, *Phys. Rev. B* **78**, 104505 (2008).
 - ¹⁴ G. Cao, C. Wang, Z. Zhu, S. Jiang, Y. Luo, S. Chi, Z. Ren, Q. Tao, Y. Wang, and Z. Xu, *Phys. Rev. B* **79**, 054521 (2009).
 - ¹⁵ H. H. Wen, G. Mu, L. Fang, H. Yang, and X. Y. Zhu, *Europhys. Lett.* **82**, 17009 (2008).
 - ¹⁶ G. Mu, L. Fang, H. Yang, X. Zhu, P. Cheng, and H. H. Wen, *J. Phys. Soc. Jpn. Suppl.* **77**, 15-18 (2008).
 - ¹⁷ G. Mu, B. Zeng, X. Zhu, F. Han, P. Cheng, B. Shen, and H. H. Wen, *Phys. Rev. B* **79**, 104501 (2009).
 - ¹⁸ K. Kasperkiewicz, J. G. Bos, A. N. Fitch, K. Prassides, and S. Margadonna, *Chem. Commun. (Cambridge)* **2009**, 707.
 - ¹⁹ N. R. Werthamer, E. Helfand and P. C. Hohenberg, *Phys. Rev.* **147**, 295 (1966).
 - ²⁰ V. Johnson, and W. Jeitschko, *J. Solid State Chem.* **11**, 161 (1974).
 - ²¹ J. Yang, X. L. Shen, W. Lu, W. Yi, Z. C. Li, Z. A. Ren, G. C. Che, X. L. Dong, L. L. Sun, F. Zhou, and Z. X. Zhao, *New J. Phys.* **11** 025005 (2009).
 - ²² H. Yang, Y. Liu, C. G. Zhuang, J. R. Shi, Y. G. Yao, S. Massidda, M. Monni, Y. Jia, X. X. Xi, Q. Li, Z. K. Liu, Q. R. Feng, H. H. Wen, *Phys. Rev. Lett.* **101**, 067001 (2008).
 - ²³ T. R. Chien, D. A. Brawner, Z. Z. Wang, and N. P. Ong, *Phys. Rev. B*, **43**, 6242-6245 (1991).
 - ²⁴ P. Quebe, L.J. Terbüchte, and W. Jeitschko, *New J. Phys.* **11** 083003 (2009).
 - ²⁵ J. Ju, Z. Li, G. Mu, H. H. Wen, K. Sato, M. Watahiki, G. Li, and K. Tanigaki, *New J. Phys.* **11** 083003 (2009).

TABLE I: Selected Rietveld refinements results of the calcium-doped $\text{Pr}_{0.87}\text{Ca}_{0.13}\text{FeAsO}$ (0.13 is the value from the refinements) at room temperature, along with that of the parent phase PrFeAsO and strontium-doped $\text{Pr}_{0.84}\text{Sr}_{0.16}\text{FeAsO}$ for comparison. The data of the latter two samples are cited from other reports.^{24,25}

sample	a (\AA)	c (\AA)	Fe-As-Fe ($^\circ$)	d_{PrOPr} (\AA)	d_{AsFeAs} (\AA)	d_{inter} (\AA)
PrFeAsO	3.985	8.595	111.968	2.405	2.690	1.750
$\text{Pr}_{0.87}\text{Ca}_{0.13}\text{FeAsO}$	3.987	8.628	112.429	2.396	2.668	1.782
$\text{Pr}_{0.84}\text{Sr}_{0.16}\text{FeAsO}$	3.985	8.622	112.413	2.387	2.666	1.785